Enhancing the numerical aperture of lenses using ZnO nanostructure-based turbid media

2013 J. Opt. 15 125714

(http://iopscience.iop.org/2040-8986/15/12/125714)

IOP Publishing Journal of Optics
J. Opt. **15** (2013) 125714 (6pp) doi:10.1088/2040-8978/15/12/125714

Enhancing the numerical aperture of lenses using ZnO nanostructure-based turbid media

Richa Khokhra[1], Manoj Kumar[2], Nitin Rawat[3], Partha Bir Barman[1], Hwanchol Jang[3], Rajesh Kumar[1,3] and Heung-No Lee[3]

[1] Jaypee University of Information Technology, Waknaghat, Solan-173234, Himachal Pradesh, India
[2] Centre for Nanotechnology, BHEL Corporate R & D, Vikasnagar, Hyderabad-500093, India
[3] Gwangju Institute of Science and Technology, Gwangju 500-712, Republic of Korea

E-mail: rajesh.kumar@juit.ac.in

Received 10 July 2013, accepted for publication 2 October 2013
Published 29 October 2013
Online at stacks.iop.org/JOpt/15/125714

Abstract
Nanosheets, nanoparticles, and microstructures of ZnO were synthesized via a wet chemical method. ZnO films with a thickness of 44–46 μm were fabricated by spray coating, and these have been investigated for their potential use in turbid lens applications. A morphology-dependent comparative study of the transmittance of ZnO turbid films was conducted. Furthermore, these ZnO turbid films were used to enhance the numerical aperture (NA) of a Nikon objective lens. The variation in NA with different morphologies was explained using size-dependent scattering by the fabricated films. A maximum NA of around 1.971 of the objective lens with a turbid film of ZnO nanosheets was achieved.

Keywords: ZnO turbid films, numerical aperture, nanosheets, nanoparticles, objective lens

1. Introduction

There are several studies on the propagation of light through scattering media to achieve better imaging/improved resolution [1–7]. On the one hand, light passing through scattering media induces wavefront distortions that degrade the image quality of optical systems [8, 9]. On the other hand, distortions induced by scattering media can be used to manipulate the wavefront in order to focus the light for better imaging [10, 11]. Recently, an enhancement of resolution by calyx-4-hydroquinone spherical nanolenses abbreviated as n-SIL (nanoscale lenses in a solid immersion lens type implementation) for near field focusing and high-resolution optical imaging beyond diffraction has also been reported [12, 13].

Solid immersion lenses, objective lenses, numerical-aperture (NA)-increasing lenses, etc, have been used to enhance the NA (i.e., the resolution) of optical microscopy [14–17]. Recently, scattering media were used by Choi *et al* [18] to overcome the diffraction limit in wide field imaging. A numerical method based on holographic imaging was used; this method converts a severely distorted image, an output from a turbid medium, into a high-resolution image. The authors called this method 'turbid lens imaging' (TLI) and demonstrated that a turbid lens applied in wide-area imaging may realize an improved spatial resolution and an enlarged field of view.

Normally, when a light ray passes through a turbid medium it bends due to scattering. This bending of light has been used to increase the NA of an objective lens. However, owing to turbidity, the image is scrambled. By applying mathematical projection operations, it was shown that the image of an object can be extracted from holographically scrambled images [18]. Thus, the turbid medium itself acts as a lens and enhances the NA of an objective lens. In the literature, gallium arsenide (GaAs) [19], titanium dioxide (TiO_2) [20], zinc oxide (ZnO) [21], and porous structures of gallium phosphide (GaP) [22], have likewise been used as light-scattering materials. However, to the best of our knowledge, mainly ZnO films have been used as random media for the focusing of light [23, 24] and as turbid lenses [18, 25] in optical imaging applications due to their

negligible absorption in the visible regime [26]. The physical reason behind using ZnO is its band gap with a value of 3.27 eV. Therefore, it does not absorb visible light and causes only bending of light rays.

For better image resolution in optical microscopy using a turbid lens, not only the NA but also the transmittance of the turbid lens should be high [18]. The greater the transmittance and bending of a turbid medium, the greater the resolution achieved in optical microscopy. A previous study by Choi *et al* [18] reported that the transmittance and the NA of a turbid lens depend on the thickness of the turbid film. In their study, only nanoparticles of ZnO were used to form turbid films and a high-resolution image was obtained by applying such a turbid film with a thickness of 25 μm and a transmission of 6%.

In the present study, we aim to demonstrate that the morphology of the ZnO structures is also an important factor when using this material in front of an objective lens in order to enhance the NA of the objective lens. Three ZnO structures, namely nanoflowers (composed of nanosheets), nanoparticles, and microstructures, were synthesized via a wet chemical method. These synthesized ZnO structures were used to fabricate turbid films by the spray-coating method. Optical experiments were performed on the thus-formed turbid films, and the corresponding transmissions of the turbid lens films were measured. Further, these turbid films were used to enhance the NA of a commercial (Nikon) objective lens. It is observed that the transmittance of the ZnO turbid films and the enhanced NA of a Nikon objective lens are dependent on the morphology and size distribution of the ZnO structures.

2. Experimental details

2.1. Synthesis of nanosheets, nanoparticles and microstructures

To synthesize nanosheets, solutions of 0.5 M $ZnCl_2$ (purity 99.99%, Sigma Aldrich) and 0.5 M NaOH (purity 98%, Merck) were prepared in distilled (DI) water. Prepared $ZnCl_2$ solution was added dropwise to the NaOH solution at 35 °C under continuous stirring for 4 h, and a white precipitate was obtained. After the reaction, the precipitate was filtered and washed several times with DI water and ethyl alcohol. To evaporate the water, the precipitate was dried for 2 h at 60 °C in a horizontal tube furnace. After drying of the above precipitate, ZnO nanosheets were obtained in bunches (called nanoflowers). In a second experiment, ZnO microstructures were formed by repeating the above experiment with a changed concentration of NaOH, i.e., 1.0 M, while keeping all the other synthesis parameters the same as in the case of the nanosheets.

Further, for the synthesis of ZnO nanoparticles, a 0.1 M solution of $ZnCl_2$ was added dropwise to 0.2 M KOH (purity 85%, Merck) solution with vigorous stirring. Then, a 0.05 M solution of cetyltrimethylammonium bromide (CTAB) (purity 99%, Sigma Aldrich) was added abruptly to the above solution. The obtained solution was stirred at 35 °C for 4 h. After 4 h, the obtained precipitate was filtered, washed several times with DI water and ethyl alcohol, and finally dried for 2 h at 60 °C to obtain ZnO nanoparticles. The morphology and structure of the synthesized ZnO materials were characterized by field emission scanning electron microscopy (FESEM) and x-ray diffraction (XRD) pattern analysis.

2.2. Turbid-film preparation

The as-synthesized ZnO structures were dissolved in C_2H_5OH solution and subsequently sonicated for 30 min to ensure a good dispersion of the ZnO particles inside of the solution and to achieve uniformity of the deposited film. Spray coating was used for the deposition of ZnO turbid films of varying thickness on glass slides. During spraying, the substrate temperature was kept at 150 °C and the heater with substrate was kept inside a fume hood to remove vapours of the solvent. The carrier gas N_2 and the ZnO solution were fed into the spray nozzle at a constant spray rate of 1 ml min^{-1}. The carrier gas flow rate was maintained at 2×10^4 kg cm^{-2}. The thickness of each film was controlled by the number of spraying cycles. The thickness of the films was measured by FESEM using cross-sectional samples. Finally, using ZnO turbid films, an experiment was performed to enhance the NA of a Nikon objective lens with a He–Ne laser ($\lambda = 632.8$ nm) of 2 mW power as light source.

3. Results and discussions

3.1. ZnO nanosheets, nanoparticles, and microstructures

Figure 1 shows an FESEM image of the bunches (nanoflowers) of synthesized ZnO nanosheets and the corresponding XRD pattern. The FESEM image at low magnification (figure 1(a)) indicates that ZnO has a dense and compact morphology consisting of micron-sized balls. From the image at higher magnification (figure 1(b)), it is observed that each individual ball has a flower-like structure with an average diameter of 2 μm. From the enlarged image, it can be seen that each flower is made up of many thin nanosheets, spreading in all possible directions (figure 1(c)). A careful examination reveals that the thickness of the nanosheets is around 10 nm and their mutual distance is more than 100 nm. Furthermore, each nanosheet has almost the same thickness perpendicular to its two-dimensional (2D) surface, indicating that the sheet growth strictly occurred within the 2D plane.

The formation of flower-like structures takes place via initially formed aggregates of ZnO nanoparticles in aqueous medium. The initially formed aggregates grow further in all possible directions and form nanosheets with the passage of time, by consuming precursor particles from the solution. In the XRD pattern shown in figure 1(d), the diffraction peaks around $2\theta = 32.7°$, 34.5°, and 36.42° correspond to the (100), (002), and (101) planes of the ZnO structure. In addition to these commonly observed orientations, weak orientations such as those corresponding to (102) and (110) are also observed in the XRD pattern at 47.44° and 56.58°, respectively. The recorded XRD pattern well matched with the reference card JCPDS 89-1397 and thus confirmed that the

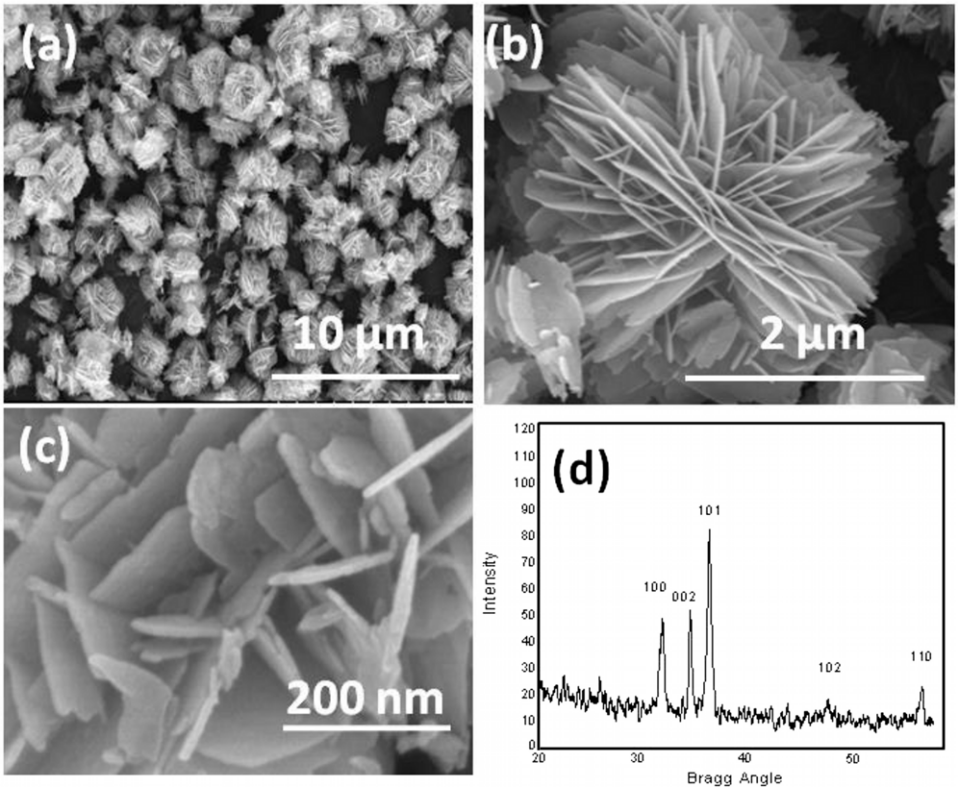

Figure 1. ZnO nanosheets formed at 60 °C for 4 h without using a surfactant. (a) FESEM image showing nanoflowers of various size, (b) FESEM image of a single nanoflower indicating a nearly parallel arrangement of nanosheets at a particular face, (c) high-magnification FESEM image of the nanosheets inside of a nanoflower, and (d) corresponding XRD pattern of the nanosheets.

nanosheets are composed of ZnO. Similar XRD results were obtained for the nanoparticles and microstructures.

The FESEM images in figures 2(a) and (b) show synthesized spherical ZnO nanoparticles with a size of 10–20 nm. During the formation of the nanoparticles, a capping material, CTAB, was used to control the growth, and therefore small-sized nanoparticles were obtained. Figures 2(c) and (d) are FESEM images of ZnO microstructures that are non-uniform and irregular.

3.2. Enhancement of the NA of a Nikon objective lens using ZnO turbid films

We attempted to enhance the NA of a Nikon objective lens using the synthesized ZnO nanosheets, nanoparticles, and microstructured turbid films. A schematic layout of the experimental setup is shown in figures 3(a) and (b). Figure 3(a) shows a schematic of experimental setup without using turbid film. The dotted lines correspond to the direction of incident laser beam at an angle (θ') greater than the acceptance angle (θ)—these rays do not enter the lens aperture. But when a turbid film is placed in front of lens (figure 3(b)) the incident laser rays at an angle θ' (greater than θ) are also bent towards the lens aperture. Therefore by using the turbid film the acceptance angle can be increased and the NA of the lens is calculated using the formula NA $= n(\sin\theta)$, where n is the refractive index of the medium—we have used $n = 2.008$ for ZnO. The transmittance of the ZnO turbid films shows an increasing trend going from nanosheets to nanoparticles and further to microstructures (figure 3(c)). The NA of a turbid lens depends on how much light is scattered upon passing through the medium. We focus on investigating the impact of different geometries of the turbid films on the NA of a Nikon objective lens. An increased acceptance angle of 79° of the objective lens is observed for a 44-μm-thick turbid film of nanosheets. The acceptance angle is 68° for a 46-μm-thick film of microstructures and 75° for a 44-μm-thick film of nanoparticles, while in air the objective lens has an acceptance angle of only 65° which corresponds to NA = 0.906 (from the relation NA $= n\sin\theta, n = 1$). In our case, the turbid film of nanosheets has a maximum acceptance angle of 79° which gives NA equal to 1.971 (taking $n = 2.008$ for ZnO). This value of the NA is obtained with a transmission of 15.23% for a 44-μm-thick turbid film of nanosheets. Similarly, NAs equal to 1.939 and 1.861 were observed with transmissions of 21.51% and 34.14% for 44-μm- and 46-μm-thick turbid films of nanoparticles and microstructures, respectively, as shown in figure 3(c).

The variation in scattering with respect to turbid films is shown in figure 4. The strength of the scattering (SC) of the turbid films composed of three different ZnO nanostructures is in the following order: $SC_{nanosheets} > SC_{nanoparticles} > SC_{microstructures}$.

We know that the scattering of light depends upon the size of the particle as well as the wavelength of the incident light. In our case, we have used laser light of wavelength

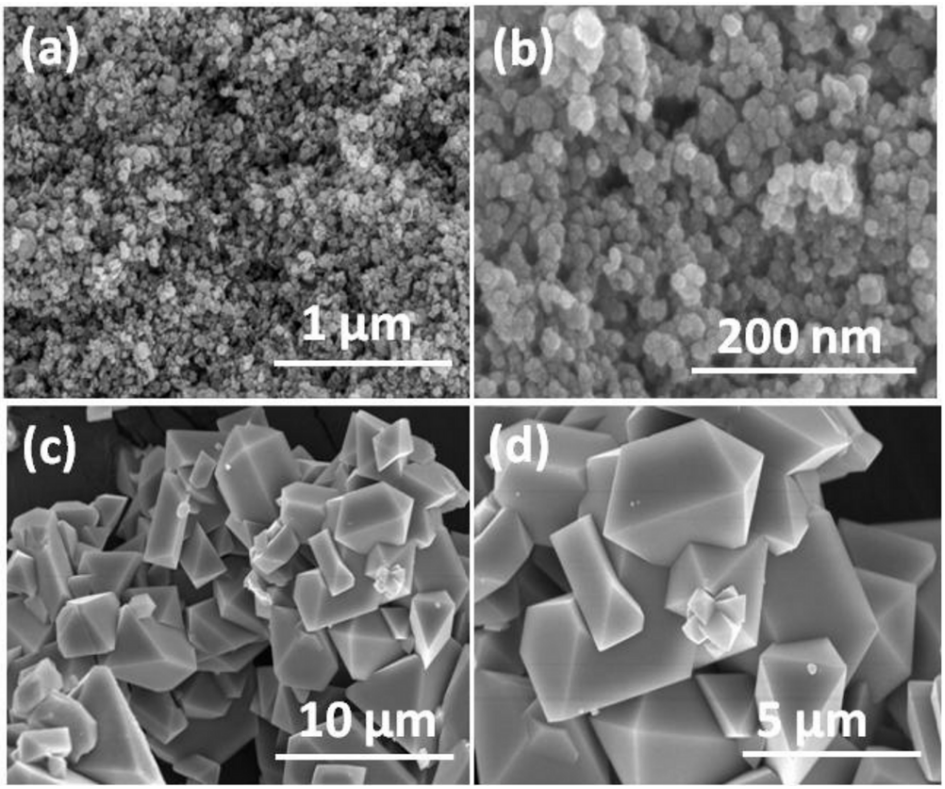

Figure 2. FESEM images of ZnO nanoparticles synthesized using CTAB as a surfactant, which controls the size of the nanoparticles. Panel (a) is an FESEM image at low magnification, whereas the FESEM image in (b) shows the uniform size distribution of the nanoparticles. Panel (c) is an FESEM image of ZnO microstructured particles formed at 60 °C for 2 h without using a surfactant, and (d) is a high-magnification FESEM image of the microstructure.

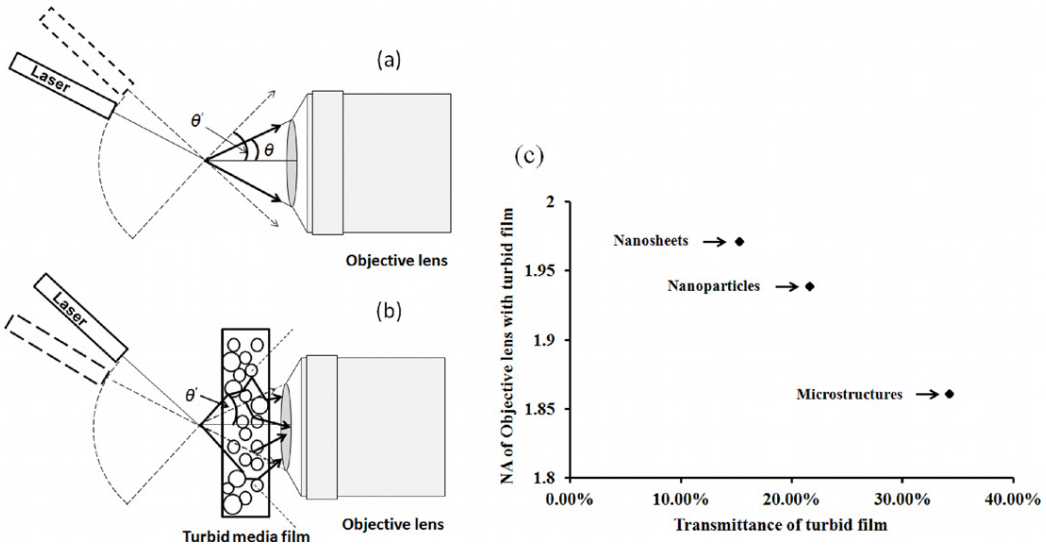

Figure 3. (a) Schematic layout of the experimental setup without using turbid film and (b) with using turbid film in front of the lens. (c) The NA of an objective lens with turbid film versus transmittance of the turbid film, plotted for the three different ZnO turbid films.

$\lambda = 632.8$ nm, therefore the scattering mainly depends upon the diameter (D) of the particles. It is well known that based upon the size parameter $x = \pi D/\lambda$ the scatterings may be explained by Rayleigh scattering ($x \ll 1$), Mie scattering ($x \sim 1$) and geometrical optics ($x \gg 1$). Since Mie scattering is applied for spherical particles [27] of size range comparable to the wavelength of incident radiation, it cannot be used for our ZnO structures as these structures do not follow the stated constraints for Mie scattering. In our case, the scattering by the films of different ZnO structure (nanoparticles, nanosheets and microstructures) can be explained by using Rayleigh scattering and geometrical optics.

We start our discussion with ZnO nanoparticles. The ZnO nanoparticles being much smaller than the wavelength

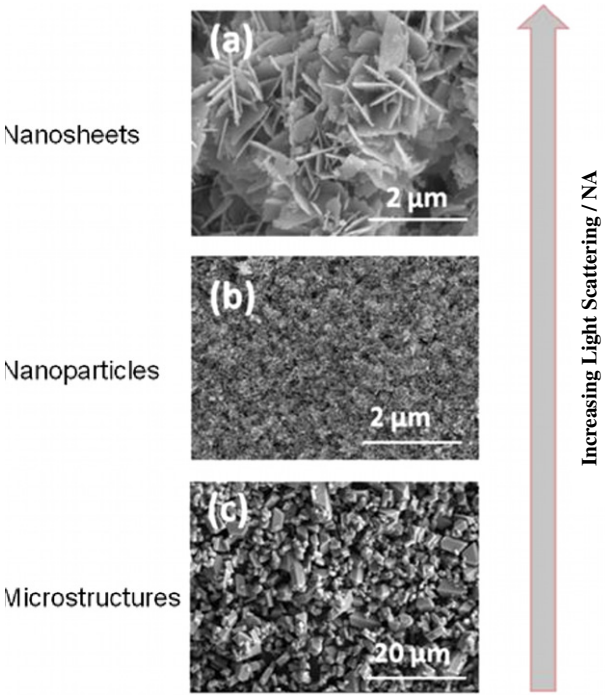

Figure 4. Light scattering originating from ZnO structures coated on a thin glass cover slip. FESEM images for (a) a turbid film of nanosheets, (b) a turbid film of nanoparticles, and (c) a turbid film of microstructures.

of incident radiation (satisfying the criterion of Rayleigh scattering, i.e. $x \ll 1$) can be considered as Rayleigh scatterers. When laser radiation is incident on the film of nanoparticles, each of the nanoparticles in the path of radiation scatters the radiation. Since the film thickness (44 μm) is much larger then the size of constituent nanoparticles, there is multiple scattering of the radiation when it passes through the film. Therefore, the overall scattering by the film can be seen as a superposition of multiple scatterings of incident radiation by nanoparticles in the film. Further, although the modelling of scattered radiation by the film of nanoparticles is complex, we can visualize the scattered radiation as composed of the contributions of many waves from oscillating dipoles [28]. Under the condition of the nanoparticle size being much smaller than the incident wavelength, the nanoparticle will be in a uniform electric field and as a whole it can be considered as an oscillating dipole [29, 30]. As the separation between the dipoles (ZnO nanoparticles) is much smaller than the incident wavelength, the phase differences are small and the collective scattering from all the dipoles occurs at larger angles in the forward direction [31]. For clarification, we consider the scattering of two dipoles. Neglecting the dipole–dipole interaction, the scattered intensity in the direction θ is given by

$$I = \text{constant}[E_1^2 + E_2^2 + 2E_1E_2\cos(\Delta\Phi)], \qquad (1)$$

where $\Delta\Phi = 2\pi r/\lambda(1 - \cos\theta)$ is the phase difference and E_1 and E_2 are the electric fields from the two dipoles. The phase difference ($\Delta\Phi$) in a particular direction θ depends upon the size parameter ($2\pi r/\lambda$). For $2\pi r/\lambda \ll 1$ (as in the case of nanoparticles), the $\Delta\Phi$ would be negligible even for larger values of θ. So the scattering in the case of nanoparticles occurs at larger angles. But in the case of $2\pi r/\lambda \sim 1$ or $2\pi r/\lambda \gg 1$, then $\Delta\Phi$ would be negligible only at smaller values of θ and hence the scattering occurs at smaller angles [31].

In the case of nanosheets, although the size of the nanosheets is large (around 2 μm wide) compared to the incident wavelength but due to their planar geometry, Mie scattering cannot be applied (since Mie theory is only applicable to spherical particles). Similarly, Fraunhofer scattering can be neglected as it occurs for particles at least 5–6 times larger than the incident wavelength [32]. Nanosheets being larger than the incident wavelength, the scattering by a nanosheet can be considered as composed of contributions of many waves generated by the oscillating dipoles that make up the nanosheet. As we know, the larger is the particle, the more radiation is scattered in the forward direction [22]. But in our experiment, we observe that the scattering angle for nanosheet film is more than that for nanoparticle film. This may be due to the contribution of specular reflections from the surface of the nanosheets. Due to the smooth surface of the nanosheets (as can be seen in the SEM image in figure 1(c)) the possibility of specular reflections cannot be neglected. And the emerging waves from the film of nanosheets can also have specular reflections at the output side of the film, contributing to the scattering angle.

Another reason for increased scattering angle in the case of nanosheets may be their morphological structure in which many nanosheets, which are often aligned in the parallel direction, are grouped in bunches. From the SEM image in figure 4(a), it is clear that there are bunches of sheets, and most of the sheets have the same parallel arrangement as that in nanoflowers even after sonication for 30 min. This is because, even after sonication, the nanoflowers do not break completely into individual nanosheets but remain in bunches when dispersed on a glass cover slip to form a turbid film. Light entering a particular area of a turbid film propagates through multiple reflections between the sheets until it meets a barrier or a normally oriented sheet within a bunch along its path. These normally oriented nanosheets in the path of light will scatter the light at higher angles than the nanoparticles due to the smaller thickness of the nanosheets, which leads to a higher value of scattering angle.

The microstructures are larger ($\sim$5 μm) than the wavelength of the light, therefore geometrical scattering can be applied. In geometrical scattering the light is prominently scattered near to the forward direction [33] and hence the scattering angle in this case is smaller as compared to nanoparticles and nanosheets.

A contribution of diffused scattering can also be deduced in our samples from the measurement of intensity of transmitted radiation. Since the films are not smooth, the incident radiation will be scattered back due to the diffused reflections. The transmittance of ZnO films is observed in the order of nanosheets < nanoparticles < microstructures. The observed smaller transmittance in the case of nanosheets is obvious since the nanosheets scatter back radiation due to the

Table 1. Transmission and NA corresponding to different morphologies of turbid films used in this work.

Structure	Thickness (μm)	Transmission of turbid film (%)	Enhanced NA of Nikon objective lens using turbid films
Nanosheets	44	15.23	1.971
Nanoparticles	44	21.51	1.939
Microstructures	46	34.14	1.861

diffused reflections as well as the specular reflections. In the case of microstructures, due to their larger size the porosity of the film is smaller as compared to the films of nanoparticles and nanosheets, and the transmittance (34.14% in case of microstructure film) will dominate in this case [34].

Table 1 shows the transmittance and enhanced NA of an objective lens coated by turbid films of different morphology. Comparing the results with the previous reported results [18] in which NA was increased from 0.15 to 0.85 for nanoparticles, our results show a better enhancement of NA (from 0.906 to 1.971) for nanosheets. Again, for better image resolution in optical microscopy using a turbid lens, not only the NA but also the transmittance of the turbid lens should be high. In our case, we have obtained a comparatively higher NA as well as transmittance for nanosheet turbid film.

4. Conclusions

In conclusion, we have shown that the NA of a Nikon objective lens can be increased for better optical imaging/improved resolution by using ZnO turbid films of different morphology. Applying ZnO turbid films, the NA of an objective lens with an initial value 0.906 could be increased to 1.861, 1.939 and 1.971 using the films composed of microstructures, nanoparticles and nanosheets, respectively (44–46 μm film thickness). The variation in NA with different morphologies was explained using a size-dependent scattering approach. The maximum NA (of 1.971) is achieved for a turbid film of ZnO nanosheets. This will result in a higher value of the NA of an objective lens with ZnO nanosheet based turbid films. The observed results also indicate that the NA of an objective lens can be further improved by fabricating thicker ZnO nanostructure film.

Acknowledgments

This work was supported by a National Research Foundation of Korea (NRF) grant funded by the Korean government (MEST) (Do-Yak Research Program, No. 2012-0005656) and the research fund of Nanotechnology Lab, Jaypee University of Information Technology, Waknaghat, Solan, India.

References

[1] Conkey D B, Caravaca-Aguirre A M and Piestun R 2012 *Opt. Express* **20** 1733–40
[2] Van Putten E G, Lagendijk A and Mosk A P 2011 *J. Opt. Soc. Am.* B **28** 1200–3
[3] Lerosey G, De Rosny J, Tourin A and Fink M 2007 *Science* **315** 1120–2
[4] Vellekoop I M and Aegerter C M 2010 *Opt. Lett.* **35** 1245–7
[5] Cui M, McDowell E J and Yang C 2009 *Appl. Phys. Lett.* **95** 123702
[6] Aulbach J, Gjonaj B, Johnson P M, Mosk A P and Lagendijk A 2011 *Phys. Rev. Lett.* **106** 103901
[7] Vellekoop I M, Lagendijk A and Mosk A P 2010 *Nature Photon.* **4** 320–2
[8] Sebbah P 2001 *Waves and Imaging Through Complex Media* (Dordrecht: Kluwer Academic)
[9] Goodman J W 2007 *Speckle Phenomena in Optics: Theory and Applications* (Englewood: Roberts & Company)
[10] Vellekoop I M and Mosk A P 2007 *Opt. Lett.* **32** 2309–11
[11] Vellekoop I M, Van Putten E G, Lagendijk A and Mosk A P 2008 *Opt. Express* **16** 67–80
[12] Lee J Y *et al* 2009 *Nature* **460** 498
[13] Mason D R, Jouravlev M V and Kim K S 2010 *Opt. Lett.* **35** 2007
[14] Kim M S, Scharf T, Haq M T, Nakagawa W and Herzig H P 2012 *Proc. SPIE* **8249** 82491B
[15] Reihani S N S, Charsooghi M A, Khalesifard H R and Golestanian R 2006 *Opt. Lett.* **31** 766–8
[16] Ippolito S B, Goldberg B B and Ünlü M S 2001 *Appl. Phys. Lett.* **78** 4071
[17] Kim M S, Scharf T, Haq M T, Nakagawa W and Herzig H P 2011 *Opt. Lett.* **36** 3930–2
[18] Choi Y, Yang T D, Fang-Yen C, Kang P, Lee K J, Dasai R R, Feld M S and Choi W 2011 *Phys. Rev. Lett.* **107** 023902
[19] Wiersma D, Bartolini P, Lagendijk A and Righini R 1997 *Nature* **390** 671
[20] Kop R H J, De Vries P, Sprik R and Lagendijk A 1997 *Phys. Rev. Lett.* **79** 4369
[21] Van Soest G 2001 *PhD Thesis* University of Amsterdam
[22] Bret B 2005 *PhD Thesis* University of Twente
[23] Popoff S M, Lerosey G, Carminati R, Fink M, Boccara A C and Gigan S 2010 *Phys. Rev. Lett.* **104** 100601
[24] Vellekoop I M and Mosk A P 2008 *Phys. Rev. Lett.* **101** 120601
[25] Choi Y, Kim M, Yoon C, Yang T D, Lee K J and Choi W 2011 *Opt. Lett.* **36** 4263–5
[26] Xu S and Wang Z L 2011 *Nano Res.* **4** 1013–98
[27] Workman J Jr and Springsteen A W 1998 *Applied Spectroscopy: A Compact Reference for Practitioners* (San Diego, CA: Academic) p 401
[28] Bohren C F and Huffman D R 1998 *Absorption and Scattering of Light by Small Particles* (*Wiley Science Paperback Series*) (Chichester: Wiley) pp 8–10
[29] Craig F, Bohren C F and Huffman D R 1983 *Absorption and Scattering of Light by Small Particles* (New York: Wiley) pp 132–4
[30] Cox A J, DeWeerd A J and Linden J 2002 *Am. J. Phys.* **70** 620
[31] Bohren C F 2001 *Clouds in a Glass of Beer: Simple Experiments in Atmospheric Physics* (New York: Dover) chapter 18, pp 271–5
[32] Stojanovic Z and Markovic S 2012 *Tech.–New Mater.* **67** 11–20 (Special Edition)
[33] Backman V, Gurjar R, Badizadegan K, Itzkan I, Dasari R R, Perelman L T and Feld M S 1999 *IEEE J. Sel. Top. Quantum Electron.* **5** 1019
[34] Stuer M, Bowen P, Cantoni M, Pecharroman C and Zhao Z 2012 *Adv. Funct. Mater.* **22** 2303–9